

Effects of phase separation and decomposition on the minority carrier diffusion length in $\text{Al}_x\text{Ga}_{1-x}\text{N}$ films

A. Cremades, M. Albrecht, J. Krinke, R. Dimitrov, M. Stutzmann et al.

Citation: *J. Appl. Phys.* **87**, 2357 (2000); doi: 10.1063/1.372187

View online: <http://dx.doi.org/10.1063/1.372187>

View Table of Contents: <http://jap.aip.org/resource/1/JAPIAU/v87/i5>

Published by the [American Institute of Physics](#).

Additional information on J. Appl. Phys.

Journal Homepage: <http://jap.aip.org/>

Journal Information: http://jap.aip.org/about/about_the_journal

Top downloads: http://jap.aip.org/features/most_downloaded

Information for Authors: <http://jap.aip.org/authors>

ADVERTISEMENT



AIP Advances

Now Indexed in Thomson Reuters Databases

Explore AIP's open access journal:

- Rapid publication
- Article-level metrics
- Post-publication rating and commenting

Effects of phase separation and decomposition on the minority carrier diffusion length in $\text{Al}_x\text{Ga}_{1-x}\text{N}$ films

A. Cremades^{a)}

Walter Schottky Institut, Technische Universität München, Am Coulombwall, 85748 Garching, Germany

M. Albrecht and J. Krinke

Institut für Werkstoffwissenschaften, Lehrstuhl VII, Universität Erlangen-Nürnberg, Cauerstr. 6, 91058 Erlangen, Germany

R. Dimitrov and M. Stutzmann

Walter Schottky Institut, Technische Universität München Am Coulombwall, 85748 Garching, Germany

H. P. Strunk

Institut für Werkstoffwissenschaften, Lehrstuhl VII, Universität Erlangen-Nürnberg, Cauerstr. 6, 91058 Erlangen, Germany

(Received 23 July 1999; accepted for publication 16 November 1999)

Combined electron beam induced current and transmission electron microscopy (TEM) measurements have been performed on both undoped and Si-doped AlGa_xN epitaxial films with aluminum contents x ranging from $x=0$ to $x=0.79$, in order to correlate the electrical and structural properties of the films. The diffusion length of holes in the films ranges between 0.3 and 15.9 μm , and the estimated lifetime of holes for doped samples varies between 0.2 ns and 16 μs . Different effects contribute to the observed increase in the diffusion length with increasing aluminum content. Among others, dislocations seem to be active as nonradiative recombination sites, and phase separation and decomposition as observed by TEM in Al-rich alloys lead to the formation of a spatially indirect recombination path due to the piezoelectric field in the films. Potential fluctuations associated with these phase irregularities could also give rise to electron induced persistent conductivity contributing to the increase of the diffusion length. From our experimental observations, we conclude that the silicon dopants are partially activated in Al-rich alloys, and do not influence significantly the values of the diffusion length of holes in these samples. © 2000 American Institute of Physics. [S0021-8979(00)00505-3]

I. INTRODUCTION

A lot of work is currently devoted to developing and improving devices based on $\text{Al}_x\text{Ga}_{1-x}\text{N}$ alloys, such as transistors¹ or UV photodetectors.² The diffusion length of carriers is a material parameter that greatly influences the performance of electronic and opto-electronic devices. In the case of GaN, only few papers³⁻⁷ report diffusion length data measured by different techniques, in the range from 0.1 to 3.4 μm depending on the carrier concentration and crystal quality. Electron beam induced current (EBIC) in the scanning electron microscope (SEM) is an established technique to measure the diffusion length of minority carriers in semiconductors.⁸ Besides, this method is able to provide spatial information, with typical resolutions of 1 μm , about the distribution of radiative and nonradiative recombination centers that locally limit the diffusion length in the film. Usually, recombination of carriers occurs at structural defects like native point defects, impurities, and extended defects (e.g., dislocations, stacking faults). Another mechanism of relevance in doped films which limits the carrier diffusion is the scattering of carriers at ionized impurities. In addition, in

the group III-nitrides internal piezoelectric fields⁹ induced by residual strain in the layer or by structural defects may perturb the electron-hole recombination dynamics¹⁰ and thus the value of the diffusion length. Recently, reported studies¹¹⁻¹⁵ are dealing with the phenomenon of persistent photoconductivity (PPC) in p -GaN, n -doped GaN, and $\text{Al}_x\text{Ga}_{1-x}\text{N}/\text{GaN}$ heterostructures. Therefore, the structural features leading to PPC must be considered in the interpretation of the diffusion length measurements.

In this work, we measure by EBIC the diffusion length of undoped and Si-doped $\text{Al}_x\text{Ga}_{1-x}\text{N}$ alloys with an aluminum content ranging from $x=0$ to $x=0.79$. We correlate the electrical and structural properties by means of transmission electron microscopy (TEM). In order to interpret the changes in diffusion length with Al content, we discuss the influence of the formation of recombination centers (mainly related to the yellow band and donor-acceptor transitions), the observed phase separation (either compositional or structural) and other structural defects such as dislocations, as well as the possible formation of metastable DX centers as one possible origin of the PPC in these samples. There are no previous reports on the diffusion length of $\text{Al}_x\text{Ga}_{1-x}\text{N}$ alloys with different Al content, and the influence of silicon doping on these films.

^{a)}Permanent address: Dpto. Física de Materiales, Facultad de Ciencias Físicas, Universidad Complutense de Madrid, 28040 Madrid, Spain; electronic mail: cremades@eucmax.sim.ucm.es

II. EXPERIMENT

Two series of undoped and Si-doped $\text{Al}_x\text{Ga}_{1-x}\text{N}$ layers were grown by plasma induced molecular-beam epitaxy (PIMBE) on *c*-plane oriented sapphire substrates. The substrate temperature was 800 °C and the growth rate 10 nm/min. In both series, the aluminum content x varied between 0 and 0.79 as determined by both x-ray spectroscopy and elastic recoil detection analysis. The doping conditions (Si cell temperature) were kept the same for all samples of the doped series. The film thickness is about 1 μm as measured by TEM. The majority carrier concentration and the mobilities in the doped samples were determined by Hall measurements at room temperature. The electron concentration ranges between 6×10^{15} and $1 \times 10^{19} \text{ cm}^{-3}$ and the corresponding mobilities were in the range of 300–10 $\text{cm}^2/\text{V s}$. The low carrier concentration present in Al-rich undoped samples does not allow Hall measurements to be carried out. The majority carrier concentration in undoped GaN is $3 \times 10^{17} \text{ cm}^{-3}$ and the electron mobility is 50 $\text{cm}^2/\text{V s}$.

The EBIC measurements have been done in a Jeol 6400 scanning electron microscope at room temperature. A proprietary computer program was used to obtain EBIC profiles using the planar metal configuration.⁸ Pt Schottky and Ti ohmic contacts were evaporated on the surface of the AlGaN layers after cleaning the specimens in acetone and dipping them in HF. From the measurements using different accelerating voltages (5, 10, 15, 20, and 25 kV), the value of 20 kV was found to minimize the influence of carrier recombination at the free surface and at the AlGaN substrate interface on the measured diffusion length. The measurements have been carried out at a low injection regime and the direct determination of the diffusion length L has been made in the range in which the distance to the contact d is larger than $2L$ ($d > 2L$). In this range, the fit to an exponential decay with the distance to the contact, d , of the EBIC current, I_{EBIC} , is accurate:⁸

$$I_{\text{EBIC}} = Ad^\alpha \exp(-d/L), \quad (1)$$

where α is assumed to be $-1/2$ corresponding to a surface recombination velocity $v_s = 0$.³ The omission of corrections to account for the film thickness leads to an underestimation of L .¹⁶

Plane-view and cross-sectional samples have been analyzed by conventional as well as by high-resolution TEM using a Philips CM 300UT (point-to-point resolution of 0.165 nm). The samples were prepared by standard techniques, involving mechanical grinding and polishing followed by 3kV Ar^+ ion-beam etching to electron transparency.

III. RESULTS AND DISCUSSION

The values of the diffusion length have been obtained as the negative inverse slope of the linear fit of $\ln(I_{\text{EBIC}}/d^{-1/2})$ versus distance d from the contact. The diffusion length ranges between 0.3 and 15.9 μm for the studied samples, as summarized in Tables I and II. The standard error of the

TABLE I. Diffusion length of minority carriers in undoped samples.

Undoped samples	$L(\mu\text{m})$
GaN	1.9
$\text{Al}_{0.27}\text{Ga}_{0.73}\text{N}$	0.3
$\text{Al}_{0.50}\text{Ga}_{0.50}\text{N}$	10.5
$\text{Al}_{0.79}\text{Ga}_{0.21}\text{N}$	5.6

diffusion length values does not exceed 3%. The relation between diffusion length L , mobility μ , and lifetime of carriers τ , is given by the equation:

$$L^2 q/kT\mu = \tau, \quad (2)$$

where q is the electron charge, k is the Boltzmann constant, and T is the temperature. From the measured value of the diffusion length and using the Hall mobilities of electrons in Eq. (2), we are able to estimate a lower limit of the lifetime of minority carriers of the doped samples, assuming that in this material system the electron mobilities are always higher than the hole mobilities. The lifetime of minority carriers (holes) varies between 0.2 ns and 16 μs for doped samples, as indicated in Table II.

In Fig. 1(a), the dependence of the diffusion length on the aluminum content in the alloys is shown for both undoped and doped samples. For doped samples, one can clearly observe an increase of the diffusion length of holes with increasing aluminum content. In the case of undoped samples, this trend is also observed, however, with some scatter. For doped samples, the diffusion length is larger than for the corresponding undoped samples, except for the $\text{Al}_{0.50}\text{Ga}_{0.50}\text{N}$ alloy. In Fig. 1(b), the dependence of L in doped samples on majority carrier concentration is shown. The decay of the diffusion length with increasing carrier concentration in the doped samples is in agreement with the scattering of carriers by ionized impurities.

Hall measurements show that the concentration of free carriers (see Table II) in doped $\text{Al}_x\text{Ga}_{1-x}\text{N}$ is reduced as the Al mole fraction increases. Similar results have been observed by Zhang *et al.*¹⁷ in the case of unintentionally doped $\text{Al}_x\text{Ga}_{1-x}\text{N}$. It has been suggested that the *n*-type conductivity exhibited by as-grown GaN should be related to N-substitutional oxygen impurities.^{18,19} A recent theoretical study about the stability of deep donor centers in GaN and AlN²⁰ concludes that oxygen is a shallow donor impurity in either cubic or wurtzite GaN, but a deep *DX* center in Al-rich $\text{Al}_x\text{Ga}_{1-x}\text{N}$ alloys. In the same article, it is reported for Si-doped samples that the calculated values for the *DX* formation energies in GaN and AlN indicate that in hexagonal

TABLE II. Electron concentration, diffusion length, and estimated lifetime of holes in doped samples.

Doped samples	$n^- (\text{cm}^{-3})$	$L(\mu\text{m})$	$\tau(\mu\text{s})$
GaN	7×10^{18}	0.4	2.2×10^{-4}
$\text{Al}_{0.25}\text{Ga}_{0.75}\text{N}$	1×10^{19}	0.5	1.5×10^{-3}
$\text{Al}_{0.50}\text{Ga}_{0.50}\text{N}$	3.5×10^{18}	6.9	2.6
$\text{Al}_{0.75}\text{Ga}_{0.25}\text{N}$	1×10^{17}	15.9	16.2

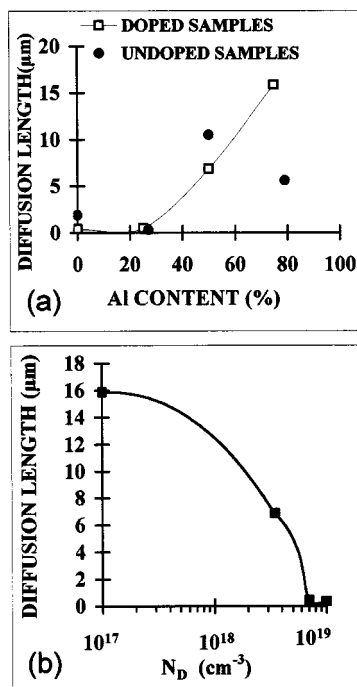


FIG. 1. Diffusion length of undoped and doped AlGaIn samples vs (a) aluminum content in the alloy and (b) electron concentration. The solid curves in the figures are guides to the eye.

$\text{Al}_x\text{Ga}_{1-x}\text{N}$ alloys, Si shallow donors should become auto-compensated by the formation of deep donors (Si:DX center) as the Al mole fraction increases. By linear interpolation, a shallow-deep transition is expected at x about 0.24 in hexagonal $\text{Al}_x\text{Ga}_{1-x}\text{N}$. This would explain the observed reduction of the number of free carriers in our doped samples, since the doping becomes ineffective with increasing Al content. Based on the same effect, it can be explained why the diffusion length is of the same order of magnitude for both undoped and doped $\text{Al}_x\text{Ga}_{1-x}\text{N}$ samples, contrary to what is expected. Therefore, the dependence of the diffusion length on the silicon doping seems to be negligible for Al-rich alloys (over 25% Al) in comparison to the influence of the structural defects that could enhance recombination processes, PPC, or trapping of carriers.

Figure 2 shows EBIC images of undoped $\text{Al}_{0.27}\text{Ga}_{0.73}\text{N}$ and doped GaN samples for illustration. The undoped sample shows a more homogeneous EBIC contrast that is slightly fluctuating [Fig. 2(a)], whereas an essentially spotty EBIC contrast consisting of bright spots of about 1 μm diameter and less surrounded by dark regions appears for the doped sample [Fig. 2(b)]. The bright areas in the EBIC images correspond to regions with a reduced density of recombination centers, while dark areas are related to regions with an enhanced density of such centers.

In order to correlate the EBIC results with the microstructure of the films, we have carried out TEM measurements on the same samples. The undoped $\text{Al}_{0.27}\text{Ga}_{0.73}$ layer [Fig. 3(a)] shows a homogeneous distribution of threading dislocations. These dislocations exclusively have line directions along the c axis. While in both samples the type and density of dislocations are similar (dislocations with Burgers

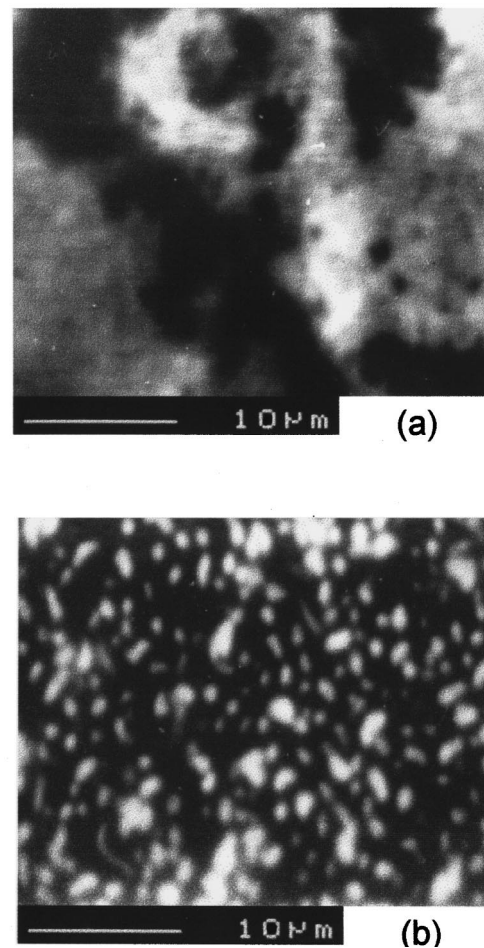
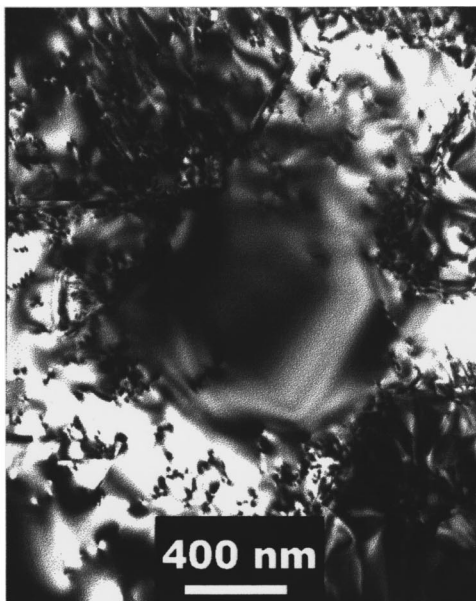


FIG. 2. EBIC images showing different defect EBIC contrast for (a) undoped $\text{Al}_{0.27}\text{Ga}_{0.73}\text{N}$, and for (b) silicon-doped GaN.

vectors $b = \langle 0001 \rangle$, $b = 1/3\langle 11-20 \rangle$, and $b = \langle 11-23 \rangle$, with a total density of $5 \times 10^9 \text{ cm}^{-2}$, the main difference consists in the arrangement of dislocations. The homogeneous distribution of dislocations allows larger diffusion lengths for carriers moving through defect free areas. In Fig. 3(b), a TEM micrograph of the doped GaN layer in plane view is shown. Hexagonal shaped regions of about 500 nm in diameter and completely free of threading dislocations are surrounded by dislocation walls with an extremely high density of threading dislocations. These dislocations are bent. Besides dislocations, planar defects lying in the basal c plane are found. These defects are also located at the border of the hexagonal regions (marked with arrows). It is interesting to note that the typical size of the hexagons corresponds very well with the size of the bright spots of our EBIC maps and the measured diffusion length for this sample (0.4 μm). We conclude that the dislocation region around the hexagonally shaped features limits the diffusion of carriers. These defect regions appear dark in the EBIC images, because of enhanced recombination at dislocations. The exact mechanism of this recombination is unclear. Since heteroepitaxial as well as single crystalline material up to now exhibits dislocation densities D in the range of $10^6 \text{ cm}^{-2} < D < 10^{10} \text{ cm}^{-2}$, the effect of defects on the diffusion length are far from clear. While according to Rosner *et al.* dislocations are recombina-



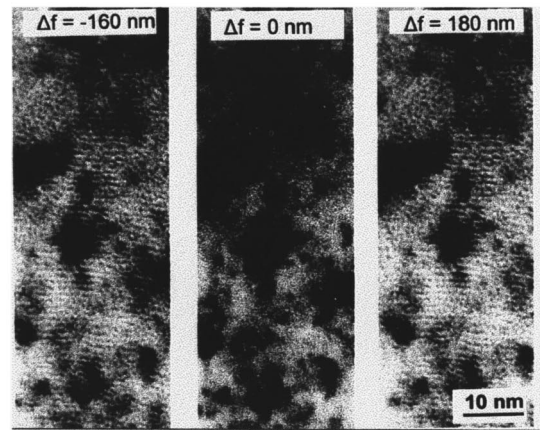
(a)



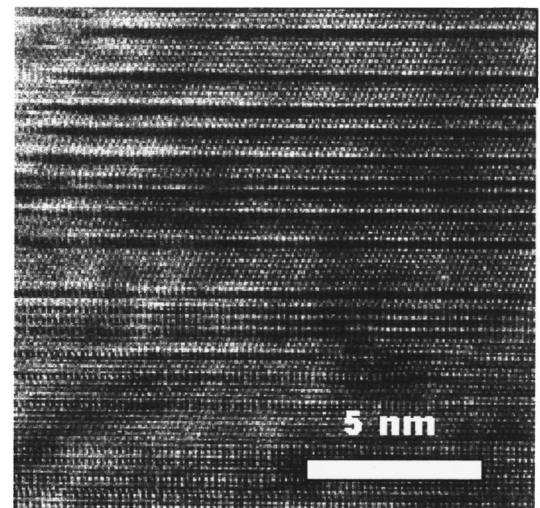
(b)

FIG. 3. Defect distribution in the layers of Fig. 2. Plane view TEM micrograph taken under [0001] multibeam conditions. (a) Undoped $\text{Al}_{0.27}\text{Ga}_{0.73}\text{N}$ layer characterized by a homogeneous distribution of dislocations. (b) Doped GaN layer, characterized by hexagonal regions completely free of defects surrounded by regions with high dislocation densities.

tion active and diffusion lengths are in the range of the average dislocation distance, others assume the diffusion length of about $0.1 \mu\text{m}$ to be an inherent property of the material that allows high dislocation densities without any significant reduction of the luminescence. Recent studies²¹ carried out by Sugahara *et al.* combining TEM and CL show direct evidence for nonradiative recombination at dislocations in GaN samples. Similar behavior of dislocations is common for other semiconductor systems.



(a)



(b)

FIG. 4. Phase separation in undoped AlGaIn. TEM micrographs were taken along the $\langle 1-120 \rangle$ zone axis. (a) Decomposition into a superstructure consisting of AlN and GaN layers with a periodicity of 1 nm in $\text{Al}_{0.5}\text{Ga}_{0.5}\text{N}$, and (b) $\text{Al}_{0.79}\text{Ga}_{0.21}\text{N}$ exhibiting a high density of cubic phase.

With increasing aluminum content in the samples phase separation (decomposition into AlN and GaN, separation into zinc blende and wurtzite phase) can be observed. TEM reveals compositional phase separation to occur in the range $0.16 < x < 0.50$, as shown in the defocus series of Fig. 4, while separation into cubic and wurtzite phase can be observed for $x > 0.50$. A periodic superstructure with a periodicity of 1 nm can be clearly resolved for the $\text{Al}_{0.50}\text{Ga}_{0.50}\text{N}$ sample. Changing the defocus of the microscope from -160 to 0 nm and finally to 180 nm exhibits a change in contrast from dark to bright stripes, going from underfocus to overfocus. At 0 defocus, the fringe pattern disappears completely. This clearly indicates a difference in inner potential due to a compositional fluctuation. In addition, cathodoluminescence reveals decomposition into pure AlN and GaN on a larger length scale.²²

An undoped sample with an Al concentration $x = 0.79$ that exhibits a high density of cubic phase is shown in Fig. 4(b). From a quantitative analysis of corresponding HRTEM images, we obtain an amount of cubic phase in the range of

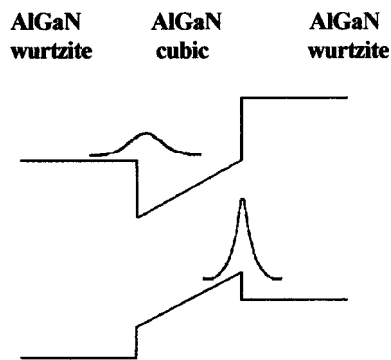


FIG. 5. Energy band scheme with electron and hole wave functions, illustrating a region of strained cubic AlGaN phase embedded in a wurtzite matrix with a piezoelectric field. The figure is not to scale, band offsets are only represented qualitatively. A similar situation is expected for chemical phase separation, with GaN embedded in the AlGaN matrix.

80% for the present sample. The wurtzite phase in this material is present exclusively in form of stacking faults incorporated into the host cubic lattice. In samples with Al content $x > 0.6$, the cubic phase is dominant and governs the optical properties. The appearance of phase separation depends strongly on the specific deposition conditions and can be largely suppressed by growing at higher substrate temperatures.

The influence of the phase separation on the diffusion length of the films could be explained as follows. The cubic phase of AlGaN is characterized by a lower band gap than the wurtzite structure. Therefore, the minority cubic phase acts as quantum wells embedded in the wurtzite matrix,²³ as illustrated in Fig. 5. Due to the piezoelectric field present in these films,^{9,10} the electron and hole wavefunctions are spatially separated (Stark effect). This separation between electron and holes results in an increased lifetime of carriers. A similar scenario can occur in the case of the chemical phase separation observed in the $\text{Al}_{0.50}\text{Ga}_{0.50}\text{N}$ layer. GaN has a lower band gap than AlN and is strained with respect to the average composition, i.e., GaN compressively, AlN tensile. Experimental evidence for this has been obtained in intentionally grown AlGaN/GaN and InGaN/GaN quantum wells structures.²⁴ This spatially indirect recombination of electrons and holes could to a large part be responsible for the unexpected high value of the diffusion length in these films, and especially for the maximum of the diffusion length shown by the undoped $\text{Al}_{0.50}\text{Ga}_{0.50}\text{N}$ layer. The estimated lifetime is of the order of μs , which is several orders of magnitude above the reported lifetimes based on photoluminescence experiments.^{25–27}

In addition, radiative recombination connected with the yellow and donor-acceptor pair luminescence increases with doping, as measured by CL,²² contributing also to the decrease of the diffusion length with increasing concentration of ionized dopants. The contribution of the observed defects acting as recombination centers is also relevant. Other results^{12,28} indicate also that the yellow luminescence is favored by Si doping, as well as other doping impurities which substitute the nitrogen site in the lattice. The origin of the yellow luminescence is not well understood and it has been

related to nitrogen vacancy $V_{\text{N-X}}$ complexes²⁹ (X are doping impurities), or to nitrogen antisite N_{Ga} ,¹² and recently to Ga-vacancy complexes $V_{\text{Ga-X}}$.

On the other hand, the formation of DX centers, responsible for the compensation of Si shallow donors in Al-rich alloys, could give rise to the phenomenon of PPC in these films.²⁰ By excitation with an electron beam of 20 kV, the same effect as detected by photoconductivity should be obtained in the presence of DX centers. The contribution of the carriers involved in this persistent electron induced conductivity process should also be detected in the EBIC measurements. An increase in the formation of DX centers with increasing aluminum content in the alloy would be in agreement with an increase of the average carrier lifetime in the film due to the persistent conductivity induced by the electron beam. Unfortunately, our experimental setup does not allow this kind of measurements to be carried out. However, photoconductivity measurements carried out on these samples³⁰ by Hirsch *et al.* show that with increasing aluminum mole fraction in the alloys the persistent photoconductivity increases by two orders of magnitude. Beside the formation of DX centers, other models have also been invoked to explain the origin for PPC in a variety of semiconductors. If carriers are spatially separated from traps by random potential fluctuations, their recapture rate at the traps can be reduced and give rise to PPC.³¹ In the AlGaN system, these kind of potential fluctuations may be caused by phase separation and phase decomposition, as observed in the TEM micrographs.

IV. CONCLUSIONS

The diffusion length of minority carriers has been measured by EBIC in planar contact configuration for undoped and silicon doped AlGaN alloys. From our observations, we conclude that the silicon doping becomes increasingly ineffective for Al-rich alloys, and therefore does not influence significantly the values of the diffusion length of holes in the doped samples in comparison with the values measured for undoped samples. Different effects contribute to the observed increase in the diffusion length with increasing aluminum content:

- (i) Structural defects, as observed by TEM. Among others, dislocations seem to be active as nonradiative recombination sites limiting the diffusion length of holes in the films, especially when dislocations are arranged in the form of walls for low aluminum contents. Other relevant effects are phase separation and phase decomposition observed in Al-rich alloys. The presence of these effects lead to spatially indirect recombination due to the piezoelectric field in the films, and therefore to an increase of the lifetime of carriers. Potential fluctuations associated with these phase fluctuations could also be the origin of an electron beam induced persistent conductivity, contributing also to the increase of the diffusion length with aluminum content in the alloys.
- (ii) Doping enhanced radiative recombination related to the yellow band as well as donor-acceptor pair recombination competes with the EBIC signal, contributing to the reduction of the diffusion length of minority carriers when

increasing the carrier concentration in the sample. For the samples with higher carrier concentration (and lower aluminum content) the scattering of carriers by ionized impurities contributes also to the observed decrease of the diffusion length.

The estimated lifetime of holes for the Al-rich samples is of the order of μs , which is several orders of magnitude above the reported lifetimes deduced from photoluminescence experiments. The increase in the lifetime by three orders of magnitude with increasing Al content is related to the existence of persistent conductivity in the samples with higher aluminum content.

ACKNOWLEDGMENTS

The authors thank Professor Piqueras for helpful discussions. A. Cremades thanks the Spanish Ministerio de Educación y Cultura for a postdoctoral grant. This work was supported by the Bayerische Forschungsförderung (FOROPTO II).

- ¹M. S. Shur, *Mater. Res. Soc. Symp. Proc.* **483**, 15 (1998).
- ²J. C. Carrano, T. Li, P. A. Grudowski, C. J. Eiting, R. D. Dupuis, and J. C. Campbell, *J. Appl. Phys.* **83**, 6148 (1998).
- ³L. Chernyak, A. Osinsky, H. Temkin, J. W. Yang, Q. Chen, and M. Asif Khan, *Appl. Phys. Lett.* **69**, 2531 (1996).
- ⁴J. W. Yang, C. J. Sun, Q. Chen, M. Z. Anwar, M. Asif Khan, S. A. Nikishin, G. A. Seryogin, A. V. Osinsky, L. Chernyak, H. Temkin, C. Hu, and S. Mahajan, *Appl. Phys. Lett.* **69**, 3566 (1996).
- ⁵S. J. Rosner, E. C. Carr, M. J. Ludowise, G. Girolani, and H. Erikson, *Appl. Phys. Lett.* **70**, 420 (1997).
- ⁶X. Zhang, P. Kung, D. Walker, J. Piortrowski, A. Rogalski, A. Saxler, and M. Razeghi, *Appl. Phys. Lett.* **67**, 2028 (1995).
- ⁷F. Binet, J. Y. Duboz, N. I. Laurent, E. Rosencher, O. Briot, and R. L. Aulombard, *J. Appl. Phys.* **81**, 6449 (1997).
- ⁸A. Jakubowich, R. Tenne, M. Wolf, A. Wold, and D. Mahalu, *Phys. Rev. B* **40**, 2992 (1989).
- ⁹M. Buongiorno Nardelli, K. Rapcewicz, and J. Bernholc, *Phys. Rev. B* **55**, 7323 (1990).
- ¹⁰M. Buongiorno Nardelli, K. Rapcewicz, and J. Bernholc, *Appl. Phys. Lett.* **71**, 3135 (1997).
- ¹¹M. T. Hirsch, J. A. Wolk, W. Walukiewicz, and E. E. Haller, *Appl. Phys. Lett.* **71**, 1098 (1997).
- ¹²H. M. Chen, Y. F. Chen, M. C. Lee, and M. S. Feng, *Phys. Rev. B* **56**, 6942 (1997).
- ¹³X. Z. Dang, C. D. Wang, E. T. Yu, K. S. Boutros, and J. M. Redwing, *Appl. Phys. Lett.* **72**, 2745 (1998).
- ¹⁴J. Z. Li, J. Y. Lin, H. X. Jiang, A. Salvador, A. Botchkarev, and H. Morkoc, *Appl. Phys. Lett.* **69**, 1474 (1996).
- ¹⁵C. Johnson, J. Y. Lin, H. X. Jiang, M. Asif Khan, and C. J. Sun, *Appl. Phys. Lett.* **68**, 1808 (1996).
- ¹⁶C. A. Dimitriadis, *J. Phys. D: Appl. Phys.* **14**, 2269 (1981).
- ¹⁷X. Zhang, P. Kung, A. Saxier, D. Walker, T. C. Wang, and M. Razeghi, *Appl. Phys. Lett.* **67**, 1745 (1995).
- ¹⁸B.-C. Chung and M. Gershenson, *J. Appl. Phys.* **72**, 651 (1992).
- ¹⁹H. Sato, T. Minami, E. Yamada, M. I. Shii, and S. Takata, *J. Appl. Phys.* **75**, 1405 (1995).
- ²⁰C. H. Park and D. J. Chadi, *Phys. Rev. B* **55**, 12995 (1997).
- ²¹T. Sugahara, H. Sato, M. Hao, Y. Naoi, S. Kurai, S. Tottori, K. Yamashita, K. Nishino, L. T. Romano, and S. Sakai, *Jpn. J. Appl. Phys., Part 2* **37**, L398 (1998).
- ²²M. Albrecht, S. Christiansen, H. P. Strunk, G. Salviati, O. Ambacher, and M. Stutzmann (unpublished).
- ²³Y. T. Rebane, Y. G. Shreter, and M. Albrecht, *Phys. Status Solidi A* **164**, 141 (1997).
- ²⁴J. S. Im, H. Kollmer, J. Off, A. Sohmer, F. Scholz, and A. Hangleiter, *Phys. Rev. B* **57**, R9435 (1998).
- ²⁵G. Mohs, B. Fluegel, H. Giessen, H. Tajalli, N. Peyghambarian, P.-C. Chin, B.-S. Philips, and M. Osinski, *Appl. Phys. Lett.* **67**, 1515 (1995).
- ²⁶J. S. Im, A. Moritz, F. Steuber, V. Härle, F. Scholz, and A. Hangleiter, *Appl. Phys. Lett.* **70**, 631 (1997).
- ²⁷J. F. Muth, J. H. Lee, I. K. Shmagin, R. M. Kolbas, H. C. Casey, Jr., B. P. Keller, U. K. Mishra, and S. P. DenBaars, *Appl. Phys. Lett.* **71**, 2572 (1997).
- ²⁸I.-H. Lee, I.-H. Choi, C. R. Lee, and S. K. Noh, *Appl. Phys. Lett.* **71**, 1359 (1997).
- ²⁹E. R. Glaser, T. A. Kennedy, K. Doverspike, L. B. Rowland, D. K. Gaskill, J. A. Freitas, M. Asif Khan, D. T. Olson, J. N. Kuznia, and D. K. Wickenden, *Phys. Rev. B* **51**, 13326 (1995).
- ³⁰O. P. Seifert, M. T. Hirsch, O. Kirfel, J. Parisi, O. Ambacher, M. Kelly, and M. Stutzmann (private communication).
- ³¹M. K. Sheinkman and A. Y. Shik, *Sov. Phys. Semicond.* **10**, 128 (1976).